

# A fundamental study of symmetrical vortex generation behind a cylinder by wake heating or by splitter plate or mesh

YASUO MORI,\* KUNIO HIJIKATA† and TAKAYOSHI NOBUHARA†

\* University of Electro-Communications, 1-5-1 Choufugaoka, Choufu City, Tokyo 182, Japan

† Tokyo Institute of Technology, 2-12-1 Ohokayama, Meguroku, Tokyo 152, Japan

**Abstract**—The mechanism of symmetrical vortex shedding behind a cylinder in a uniform, upward flow by heating the wake with fine wires or by using a splitter plate or mesh is experimentally studied. In the case of heating the wake the vortices are gradually modified from Karman vortex streets to symmetrical vortices with increase of heat input. Similar symmetrical vortex shedding is also observed by increase of the splitter plate length or mesh number behind the cylinder. An eigenfrequency of symmetrical vortex shedding is experimentally determined and is explained by an instability of the shear layer separation at the side of the cylinder.

## 1. INTRODUCTION

IT IS well known that asymmetrical (Karman) vortices are generated behind a cylinder of diameter  $d$  located in a uniform flow  $U_0$ . The regular Karman vortex streets are observed when Reynolds number  $Re = U_0 d / \nu$  is in the range 60–5000. The Strouhal number  $St = fd / U_0$  is nearly constant in that Reynolds number region, where  $f$  is a vortex shedding frequency.

In a premixed flame, however, symmetrical vortex streets can be observed behind the cylindrical horizontal flame holder [1]. Figure 1 is a shadowgraph of a premixed flame held by a cooled, horizontal cylinder of 3 mm O.D., where the upward velocity of the mixture of city-gas and air is  $3.5 \text{ m s}^{-1}$ . The symmetrical vortex streets can be clearly seen in the flame. Not only in a premixed flame but also in a diffusion flame, steady and stable symmetrical vortices can be observed instead of the Karman vortex streets. However, systematic investigations of such symmetrical vortex streets have been done infrequently and the flow characteristics and mechanism of symmetrical vortex generation have not been clarified.

Symmetrical vortex streets can also be observed in the wake of a cylinder with a splitter plate at the centerline of the wake [2]. However, most investigations about the flow around a cylinder with a splitter plate have been carried out in the light of the wake control but have not discussed the mechanism of symmetrical vortex shedding.

Symmetrical vortex shedding in the combustion process behind a cylindrical flame holder is considered to be attributed to heat release, material change by chemical reactions, buoyancy force caused by the heat release and other factors. In a preparatory experiment, it was clarified that the first two of these phenomena did not directly affect the symmetrical vortex shedding but that the buoyancy force did. This can be understood from comparison of the two photo-

graphs of Figs. 1 and 2. In Fig. 2, the streamlines behind a 12-mm-O.D. cylinder in a uniform, upward flow are visualized by a smoke-wire method, where the wake is electrically heated by fine wires connected in series and located in parallel with the cylinder axis at the center of the wake. Symmetrical vortex streets are clearly seen and are quite similar to Fig. 1.

Thus, the symmetrical flames behind the cylinder motivated the study of the symmetrical vortex shedding by heating the wake and also by use of a splitter plate or mesh. The effect of heating the wake was studied by changing the total heat input and the cylinder diameter. In the case of the splitter plate or

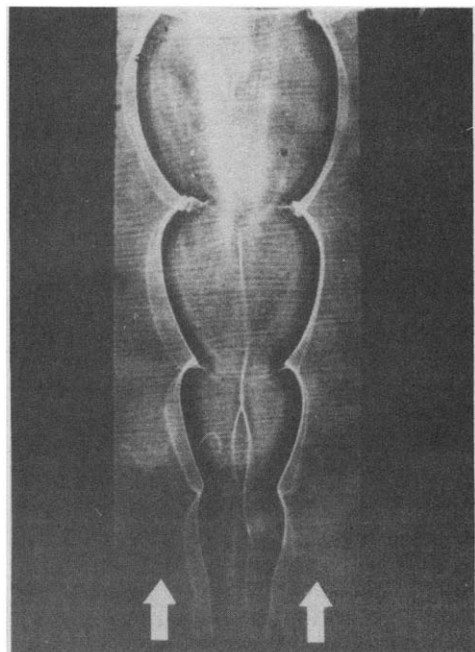


FIG. 1. Symmetrical vortex streets in the premixed flame.

## NOMENCLATURE

$d$	diameter of cylinder [m]	$\sqrt{t^2}$	r.m.s. value of temperature fluctuation [°C]
$f$	frequency of vortex shedding [Hz]	$U_0$	oncoming uniform velocity [m s <sup>-1</sup> ]
$f_{in}$	frequency of external acoustic excitation [Hz]	$u$	fluctuating velocity component of $X$ direction [m s <sup>-1</sup> ]
$l$	length of splitter plate or mesh [m]	$\sqrt{u^2}$	r.m.s. value of velocity fluctuation [m s <sup>-1</sup> ]
$Q$	heat input in wake per unit length of cylinder [W m <sup>-1</sup> ]	$Re$	Reynolds number $U_0 d/\nu$
$q$	input heat flux [W m <sup>-2</sup> ]	$St$	Strouhal number, $fd/U_0$
$T$	time mean temperature [°C]	$X$	main flow direction [m]
$t$	fluctuating component of temperature [°C]	$Y$	direction perpendicular to $X$ [m].

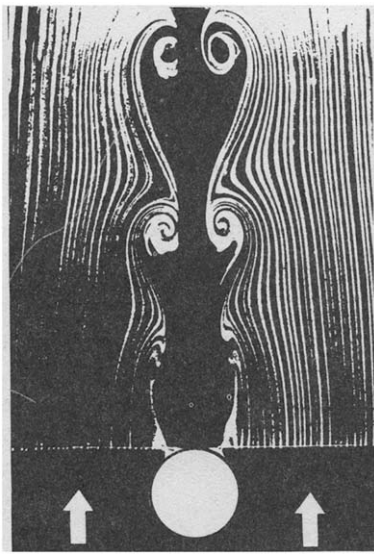


FIG. 2. Symmetrical vortex streets by heating the wake.

mesh, the effects of plate length, mesh number and shape of obstacle on the vortex performance were investigated.

The frequency of the symmetrical vortex shedding was measured and compared with that of the free separated shear layer from the cylinder. These results prove that the symmetrical vortex shedding is initiated by the free separated shear layer because the buoyancy force or the splitter plate prevents the interaction between both side shear layers and suppresses the transverse motion of fluid across the centerline of the wake behind the cylinder.

## 2. EXPERIMENTAL APPARATUS

A schematic diagram of the experimental apparatus is shown in Fig. 3. Air from a blower goes through an orifice meter, a settling chamber and a test section. The test section of the wind tunnel was a square of 120 mm a side and the walls were made of acrylic resin

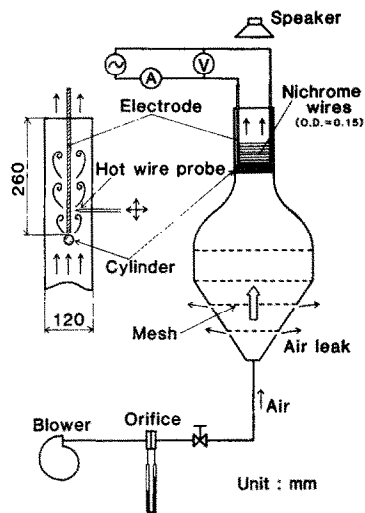


FIG. 3. A schematic diagram of the experimental apparatus.

for visualization by a smoke-wire method. A cylinder was placed horizontally and perpendicularly to the upward, uniform flow 40 mm downstream from the inlet of the wind tunnel. Mean and fluctuation components of the velocity and the temperature were measured by hot and cold wires of 5  $\mu$ m tungsten, respectively, and analyzed by a FFT.

Since the free-stream turbulence in the oncoming flow largely affects the performance of vortex shedding, the wind tunnel was constructed to have a low turbulence intensity. However, the flow had a dominant frequency component of 25 Hz caused mainly by acoustic resonance of the settling chamber. In order to eliminate this disturbance the test section was mechanically insulated by rubber sheets and a small amount of the air flow was leaked at the inlet of the chamber to avoid the acoustic resonance. For precise measurements of an eigenfrequency of vortex shedding, an acoustic excitation was made by a speaker downstream of the wind tunnel. The eigenfrequency was determined from the measurement of the maximum amplitude of temperature or velocity

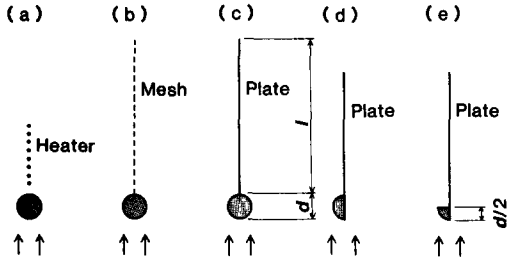


FIG. 4. Methods of wake control.

fluctuation by changing the frequency of acoustic excitation.

Fine wire heaters, a splitter mesh and a plate were used as wake control methods. In addition to these experiments, a semi- and a quarter-cylinder as shown in Fig. 4 were used instead of a circular cylinder to examine the vortex shedding. The detail structure of the heater for heating wake is shown in Fig. 5. Ten fine resistance wires of 150  $\mu\text{m}$  O.D. were positioned horizontally between two copper electrodes. The distance between the fine wires was 3 mm and the total length of the heating region was 27 mm. The wires were electrically heated and the heat input per unit length  $Q$  was calculated from the supplied voltage and current. In order to check the effect on the wake of installing fine wires, the wake flow pattern was visualized without heating the wires. Asymmetric Karman vortex streets were observed, confirming that the heating device has no effect on the wake performance under the no-heating condition.

In the case of heating the wake, it is expected that the plane on the centerline of the wake prevents the interaction between the two shear layers formed by the flow separation from the cylinder surface. In order

to extend this fact, a plate-shaped mesh was adopted as a wake splitter, where both shear layers can hardly interact with each other across the mesh. The length of the mesh was over 6 times the cylinder diameter and the numbers of mesh used were 20, 30 and 40. The flow resistance coefficient across the 40 mesh was 1.6 times larger than that across the 20 mesh.

In the first experiment, the splitter plate was used in order to prevent completely the interaction of two shear layers. The plate length was changed from 4 to 8 times the cylinder diameter. Four kinds of cylinder were used, the diameters of which were 8, 12, 24 and 30 mm, respectively. A semi-cylinder with a splitter plate, as shown in Fig. 4(d), was also adopted in order to compare the frequency of the shedding vortex with that of the full cylinder as the test obstacle.

Since the separation point of the cylinder was almost  $90^\circ$  from the stagnation point, a quarter-cylinder with a splitter plate, as shown in Fig. 4(e), was made and the frequency of the shedding vortices was also tested. The eigenfrequency of shedding vortex was compared with those of the cylinder and the semi-cylinder.

### 3. SYMMETRICAL VORTEX SHEDDING BY HEATING WAKE

The wake flow patterns taken when heating the wake with fine wires are shown in Fig. 6. For both cases, the uniform oncoming velocity was  $0.61 \text{ m s}^{-1}$ , the cylinder diameter was 12 mm, the Reynolds number was 490 and the flow was excited by sound of 16 Hz. Only the heat flux was different. Under the no-heating wake condition, Karman vortex streets were observed. With increase of the heat input, the wake pattern was changed from asymmetrical to symmetrical. In Fig. 6(b) the symmetrical flow pattern

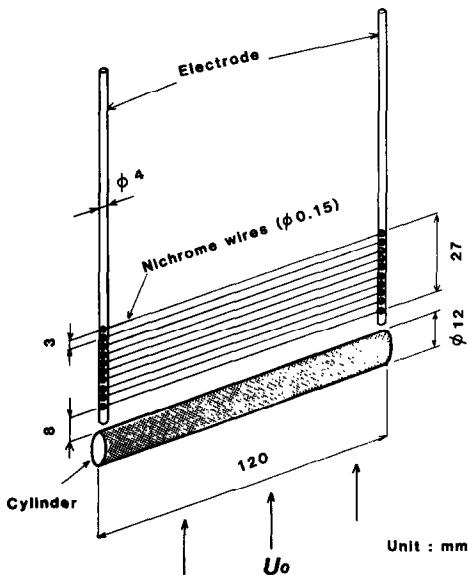


FIG. 5. Apparatus of heating a cylinder wake.

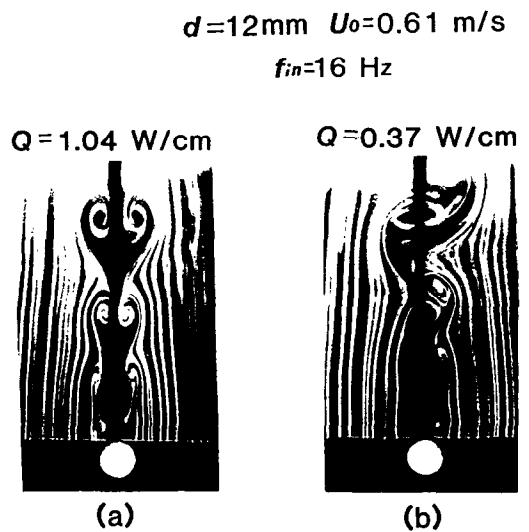


FIG. 6. Vortex streets behind a cylinder under different heat flux conditions of wake heating.

can be observed just behind the cylinder but, going downstream, the asymmetrical component is amplified and Karman vortex streets are formed. However, for higher heat input into wires, the wake pattern remains symmetric as shown in Fig. 6(a). In the far downstream region, transition from symmetrical to asymmetrical vortices is observed, since the asymmetrical vortex streets are more stable than the symmetrical ones in the uniform flow.

In the case of no wake heating, pressure fluctuation caused by the asymmetrical vortex streets existing downstream brings about the periodic movement of the stagnation point and promotes asymmetrical vortex shedding from the cylinder. However, by heating the center region of the wake near the cylinder, the strong buoyancy force prevents transverse flow across the centerline, thus the stagnation point comes to a standstill. This is the cause of generating the asymmetrical vortex streets downstream of the cylinder.

Frequency performance of the symmetrical vortex by wake heating was measured by using the r.m.s. value of the temperature fluctuation and the results are shown in Fig. 7. The temperature fluctuation becomes maximum when the exciting frequency is 20 Hz. In this condition, the components—except 20 Hz—could not be detected and the wake flow pattern was quite plane symmetric. Departure from this frequency brought about a decrease in the amplitude of temperature fluctuation. When the excitation frequency was 10 or 30 Hz, the vortex shedding did not synchronize with the excitation and the periodicity disappeared. From these observations, it may be concluded that the vortex shedding resonates with the external excitation at the frequency having the maximum amplitude of the temperature fluctuation; this frequency is called the eigenfrequency of symmetrical vortex shedding.

The variation of the eigenfrequency is shown in Fig. 8 by changing the oncoming velocity and the heating flux  $q$ . The lower limits of solid lines in the figure, that is the left end, show the limit of symmetrical vortex shedding. In the region of the dotted line, vortices not having a symmetrical structure can be observed. The

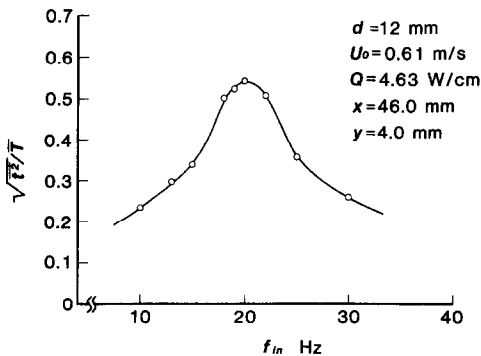


FIG. 7. Intensity of temperature fluctuation against external excitation frequency under the symmetrical vortex shedding condition by wake heating.

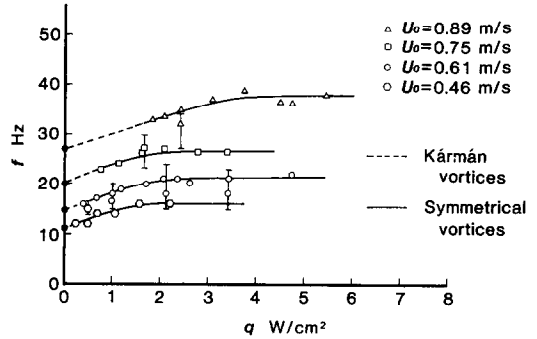


FIG. 8. Eigenfrequency of symmetrical vortex shedding by wake heating.

eigenfrequency of the symmetrical vortex generation depends weakly on the heat flux and becomes constant in the high heat flux region. In the figure, the data without external excitation are shown by the same symbols but with the vertical line, whose length indicates the variation range of the datum. Under the no external excitation condition, the frequency range of the vortex shedding widens due to surrounding disturbance, but the mean value is considered to be the same as the one with excitation. Values extrapolated to the zero-heating condition, shown by solid circles in the figure, give the eigenfrequency of imaginary symmetrical vortex shedding without the secondary effects of heating caused by the buoyancy force. These data can be compared with those obtained by use of splitter plates.

#### 4. SYMMETRICAL VORTEX SHEDDING BY SPLITTER PLATE

The cause of symmetrical vortex shedding by wake heating is considered to be the fact that the buoyancy force prevents the interaction between two vortex streets, where asymmetrical vortex streets far downstream of the cylinder can not affect the fluctuation of the separation and the stagnation points. In order to confirm the mechanism proposed above in relation to symmetrical vortex shedding, results of the wake heating by fine wires are compared with those by the splitter plate and mesh.

Firstly, the performance of the wake of the cylinder having a splitter plate as shown in Fig. 4(c) was examined. In the case of the splitter plate or mesh, the flow characteristic was measured by hot-wire anemometers. Figure 9 shows a cross correlation of two hot-wire signals which were located at the symmetrical point of the wake at nearly  $2d$  downstream of the cylinder, where the center of the shear layer is. The cylinder diameter  $d$  was 12 mm, the uniform oncoming velocity was  $U_0 = 0.75 \text{ m s}^{-1}$ , the length of the plate  $l$  was  $6d$ . The cross correlation is maximum at  $\tau = 0$  and its profile against  $\tau$  is nearly sinusoidal, which means that the behaviors of the two shear layers is symmetric and periodic. The frequency of this periodic phenomenon is 22 Hz. By decreasing the length

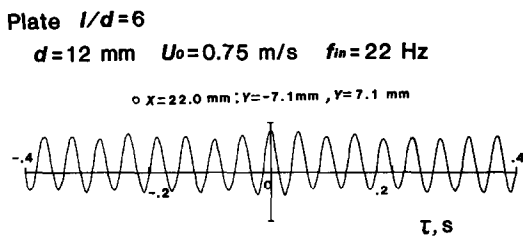


FIG. 9. Cross correlation of the velocity fluctuations at the symmetrical points against the centerline of the wake with the splitter plate.

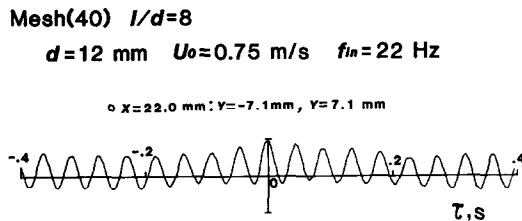


FIG. 11. Cross correlation of the velocity fluctuations at the symmetrical points against the centerline of the wake with the splitter mesh.

of the splitter plate under the constant external exciting frequency of 22 Hz, the intensity of the fluctuation component of 22 Hz decreased. When  $l/d = 2$ , the maximum frequency component of the cross correlation became 13 Hz and its value at  $\tau = 0$  was negative, which indicated asymmetrical behavior of the two shear layers. Of course, Karman vortex streets of 12 Hz were detected under the  $l = 0$  condition.

From these results, it is concluded that symmetrical vortex shedding occurs when the plate length is sufficiently long and that the frequency of vortex shedding synchronizes well with the external excitation. In Fig. 10, the fluctuation velocity intensity is plotted against the external excitation frequency under the same condition as in Fig. 9, where the intensity has a peak at 22 Hz. By using this method, dependency of the eigenfrequency upon the oncoming velocity and the cylinder diameter were obtained.

Secondly, the flow characteristic around the cylinder with a splitter mesh was investigated. In the case of the mesh number of 20, the flow pattern in the wake showed behavior similar to heating the wake at low heat input, namely the shedding vortices were asymmetric, even if the mesh length is long. When the mesh number was 30, symmetrical vortex shedding was observed, but the transition to the asymmetrical condition occurred  $2d$  downstream of the cylinder. On the other hand, when the mesh number was 40, only symmetrical vortex streets could be detected in the

whole region where the mesh existed. In Fig. 11, the cross correlation of the velocity signals obtained by two hot-wire anemometers for the splitter mesh of  $l/d = 8$  is shown, which was obtained under the same condition as Fig. 9. It is quite similar to that for the splitter plate but the intensity is a little lower. Therefore, it is shown that the splitter mesh can play the same role as the plate, even though it does not fully interrupt the cross flow through it. By changing the oncoming velocity, the eigenfrequencies of the symmetrical vortex shedding for the splitter plate and mesh were measured and plotted in Fig. 12, where the diameter of the cylinder is 12 mm. Data for the splitter mesh of 40 and the plate exit fall on the same straight line which shows that  $f$  is proportional to  $U_0^{3/2}$ . In the figure, results for no external excitation of the splitter plate are shown by the circles with the vertical bars. The length of the bar indicates the half width of the frequency spectrum of the velocity fluctuation. This result shows that the perfect shield of the two shear layers of the cylinder, such as a splitter plate, is not necessary for formation of the symmetrical vortices, but prevention of the crossing flow at the wake centerline is required.

The frequency dependency of the shedding, symmetrical vortices upon the velocity is different from that of Karman vortices. Therefore, the generation mechanism of the symmetrical vortex streets is considered to be different and the cause of the eigenfrequency must be discussed. For this purpose the

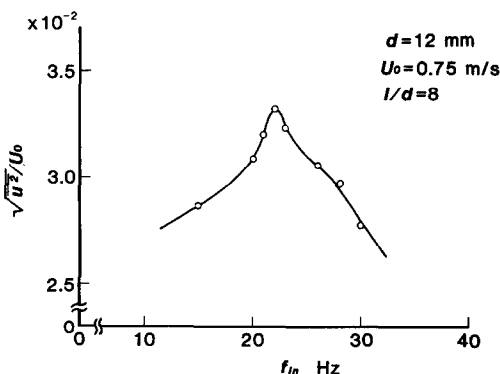


FIG. 10. Intensity of the velocity fluctuation against external excitation frequency under the symmetrical vortex shedding condition by the splitter plate.

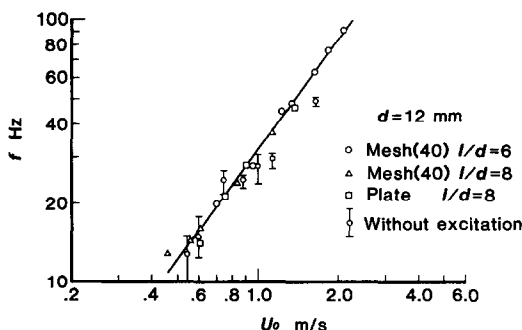


FIG. 12. Relation between the eigenfrequency of symmetrical vortex shedding and the uniform oncoming velocity to the cylinder.

frequency performance of the wake of a semi-cylinder with splitter plate, as shown in Fig. 4(d), was investigated. In this case, only one free shear layer exists and the interaction of shear layers can never occur. The eigenfrequency of the semi-cylinder agreed with that of the circular cylinder with splitter plate as shown below. This means that the eigenfrequency is controlled by the instability performance of the shear layer itself. As far as the eigenfrequency only depends on the shear layer, it may be considered that the rear half of the cylinder could not have much effect on the frequency. The wake of quarter-cylinder with the splitter plate as shown in Fig.4(e) was examined. This experiment has the other advantage that the velocity profile and its development along the flow direction can be measured exactly. The eigenfrequency for the quarter-cylinder was also found to be proportional to  $U_0^{3/2}$  and agreed with those of the semi-circular and circular cylinders.

It has been clarified that the dependency of the eigenfrequency upon the oncoming velocity  $U_0$  has the 3/2 power for all cases of the cylinders with splitter plate, mesh and of the semi- and the quarter-cylinder with the splitter plate. Concerning the characteristic length of the vortex shedding phenomenon, the length of the splitter plate is not important, because the eigenfrequency does not depend on it, if the plate is sufficiently long. The thickness of the laminar boundary layer just before the separation point is the most important, and this is determined from the oncoming velocity and the cylinder diameter. Therefore, the cylinder diameter is considered as the characteristic length of the symmetrical vortex shedding phenomena.

From the experimental results stated above,  $f$  is shown to be inversely proportional to the square root of the cylinder diameter  $d$  and is expressed as

$$f = \text{const.} \times U_0^{3/2} / d^{1/2}. \quad (1)$$

By using the nondimensional variables of Reynolds number  $Re = U_0 d / \nu$  and Strouhal number  $St = f d / U_0$ , the frequency of the symmetrical vortex shedding given by equation (1) is rewritten as follows

$$St = \text{const.} \times Re^{1/2}. \quad (2)$$

The experiment relations between  $Re$  and  $St$  for the splitter plate and mesh are plotted in Fig. 13. Results for Karman vortex streets, obtained from the experiment without splitter plates, are also shown in the figure, where the Strouhal number is nearly constant (with a value of 0.21) as is well known. This figure clearly shows that the generation mechanisms of the symmetrical and the asymmetrical vortices are quite different.

### 5. PREDICTION OF VORTEX SHEDDING FREQUENCY

It has been reported that the free shear layer is unstable and that the neutral stability curve predicts

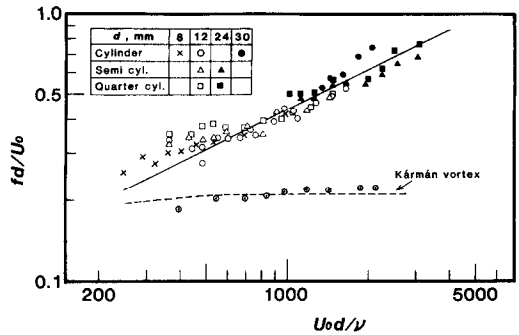


FIG. 13. Relation between the Strouhal number of symmetrical vortex shedding and the Reynolds number for circular, semi- and quarter-cylinder with splitter plate or mesh.

the eigenfrequency. As reported, the eigenfrequency of the free shear layer behind the backward step is determined by the velocity of the main flow and the wall length before the separation point, which decides the initial thickness of the shear layer [3]. In cases of the two-dimensional or axisymmetric jets into a stagnant fluid having a uniform velocity  $U_0$  at the nozzle exit, the eigenfrequency is known to be proportional to 3/2 power of  $U_0$  [4, 5]. Anyway, the eigenfrequencies of these instabilities are predicted by the linear instability theory [6].

In order to clarify the relation between the frequency of the symmetrical vortex shedding from a cylinder by the wake control and that predicted by the linear instability theory of the free shear layer, the velocity profile just downstream of the separation point must be known. Such profiles behind the cylinder are very difficult to measure because of the unsteady fluctuation of the separation point and the existence of the rear half of the cylinder, but those behind the quarter-cylinder are easy to measure and the results are shown in Fig. 14. The velocity was

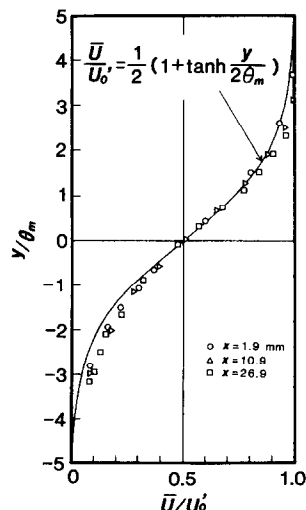


FIG. 14. Velocity profile in the separated shear layer of a quarter-cylinder with the splitter plate.

made nondimensional by the outer velocity of the shear layer  $U_0'$  but not the oncoming velocity  $U_0$ , because  $U_0'$  was not equal to  $U_0$  and slightly accelerated to the separation point. The distance perpendicular to the main flow was made nondimensional by the momentum thickness of the shear layer  $\theta_m$ , when the diameter of the quarter cylinder is 24 mm.

The experimental results agree well with the solid line of the hyperbolic tangent curve which are well known for the backward step. In the case of the backward step, the frequency having the maximum growth rate for the small amplitude disturbance has been reported as follows [4, 7]

$$f = 0.0164U_0'/\theta_m \tag{3}$$

However, a direct comparison of our data to the above equation is not preferable and some modification is needed as discussed below.

In case of the instability analysis of the backward step flow, the momentum thickness does not change along the flow direction. On the other hand, in the separated flow behind the circular cylinder or even in that of the quarter cylinder, the momentum thickness does change along the flow direction, due to the pressure variation after the separation point. In Fig. 15, variations of the momentum thickness after the separation are plotted for the quarter-cylinders of 12 and 24 mm, where the uniform oncoming velocity to the cylinder is  $0.75 \text{ m s}^{-1}$ . The momentum thicknesses increase and approach the constant values, then increase again. The initial increase of the momentum thickness is brought about by the effect of the pressure variation upstream of the separation and the second increase is caused by the transition from laminar to turbulent flow and by the effect of the splitter plate.

In the experiment, only one eigenfrequency can be detected in the region where the momentum thickness is nearly constant and the flow is laminar. When the external velocity of the shear layer  $U_0'$  and the local momentum thickness  $\theta_m$  are used in equation (3), the predicted values of eigenfrequency for quarter-cylinders of 12 and 24 mm are 24 and 16.4 Hz, and agree

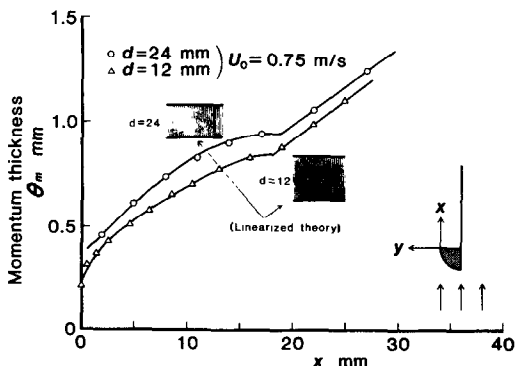


FIG. 15. Distribution of the momentum thickness along the shear layer.

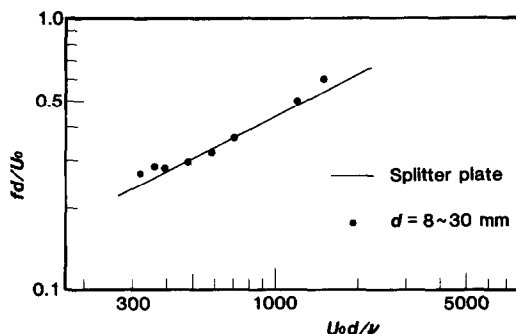


FIG. 16. Relation between the Strouhal number of symmetrical vortex shedding and the Reynolds number for wake heating.

well with the experimental results of 22 and 15.6 Hz, respectively. These discussions lead to the conclusion that the eigenfrequency of the symmetrical vortex is closely connected with the instability frequency of the shear layer of the separated flow. The splitter plate or mesh controls the crossing flow at the centerline of the wake, depresses the effect of Karman vortex and makes the effect of shear layer instability predominate.

Since the mechanism of symmetrical vortex shedding for the heating wake is considered to be the same as that for the splitter plate, the Strouhal number for the heating wake is compared with those of the splitter plate in Fig. 16. In order to eliminate the buoyancy effect of heating, the eigenfrequency extrapolated from the broken line to the zero heat input as shown in Fig. 8 is used for comparison. Results for the heating wake are shown by solid circles and the solid line is the result for the splitter plate. The agreement between them means that the mechanism of symmetrical vortex shedding is the same for both cases.

### 6. DISCUSSION ABOUT VORTICES IN FLAME

The most dominant frequencies of temperature fluctuation in the diffusion and premixed flames where the symmetrical vortex streets were observed are shown in Fig. 17. Results for symmetrical vortex shed-

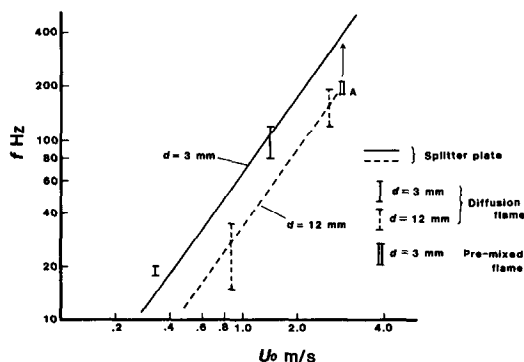


FIG. 17. Frequency of symmetrical vortex shedding in flame against the uniform velocity.

ding from the cylinder with a splitter plate or mesh given above are also plotted in the figure. There is no external acoustic excitation in the combustion experiments. As shown in Fig. 1, the symmetrical vortex streets in the flame are elongated along the flow direction due to the flow acceleration by expansion due to combustion. Therefore, the temperature fluctuations were detected just behind the cylindrical flame holder and the mean oncoming velocity was used in the figure. The result of Fig. 1 for the premixed flame is indicated by the point A in Fig. 17 whose flame holder was a 3-mm-O.D. cylinder. Other results were obtained in diffusion flames. The results for the splitter plate (shown by lines) well explained those for the diffusion flame but are slightly higher than that of the premixed flame. These differences are thought to be brought about by the effect of diverging streamlines due to the combustion as noted above. Therefore, it is concluded that the symmetrical vortex shedding in the flame is also caused by the same mechanism as the case of the splitter plate.

## 7. CONCLUSIONS

By considering the fact that the asymmetrical vortices, i.e. Karman vortex streets, cannot be observed in the wake of a flame held by in a cylindrical flame holder, cases of forming symmetrical vortex streets by use of hot, fine wires, splitter plates, meshes and others are experimentally investigated and the mechanism of symmetrical vortex shedding is discussed. The following conclusions are obtained.

1. Symmetrical vortices can be generated when the feedback effect of the flow field fluctuation caused by the Karman vortex streets on the flow just

downstream of the cylinder is negligible due to buoyancy and to the existence of the splitter plate or mesh.

2. The Strouhal number of the symmetrical vortex shedding is proportional to the square root of the Reynolds number.
3. The shedding of the symmetrical vortices is caused by the instability of the free shear layer just behind the separation point.
4. The symmetrical vortex streets in the flame are also explained by the same mechanism in the case of heating the wake and use of the splitter plate.

*Acknowledgement*—The authors gratefully acknowledge Associate Professor Toshio Miyaushu for his support in the field of combustion.

## REFERENCES

1. Y. Mori, T. Miyauchi and I. Yamasaki, Fundamental study on pseudo-turbulent flames, *Trans. Japan Soc. mech. Engrs* (in Japanese) **50**, 2228–2237 (1984).
2. D. J. Apelt, G. S. West and A. A. Szewczyk, The effects of wake splitter plates on the flow past a circular cylinder in the range  $10^4 < Re < 5 \times 10^5$  *J. Fluid Mech* **61**, 187–198 (1973).
3. H. Sato, Experimental investigation on the transition of laminar separated layer, *J. phys. Soc. Japan* **11**, 702–709 (1956).
4. P. Freymuth, On transition in a separated laminar boundary layer, *J. Fluid Mech.* **25**, 683–704 (1966).
5. H. Sato, The stability and transition of a two-dimensional jet, *J. Fluid Mech.* **7**, 53–80 (1960).
6. I. Tani, *Progress in Fluid Mechanics, 'Turbulence'* (in Japanese). Maruzen, Tokyo (1980).
7. A. Michalke, On the inviscid instability of the hyperbolic-tangent velocity profile, *J. Fluid Mech.* **19**, 543–556 (1964).

## ETUDE FONDAMENTALE DES TOURBILLONS SYMETRIQUES DERRIERE UN CYLINDRE, PAR CHAUFFAGE DU SILLAGE OU PAR PLAN SEPARATEUR

**Résumé**—On étudie le mécanisme de séparation des tourbillons symétriques derrière un cylindre dans un écoulement ascendant uniforme par chauffage du sillage avec des fils fins ou avec un plan séparateur ou une grille. Dans le cas du chauffage du sillage, des tourbillons sont graduellement modifiés depuis l'allée de tourbillons de Karman jusqu'aux tourbillons symétriques en augmentant l'apport de chaleur. On observe un aspect similaire en augmentant la longueur du plan séparateur ou le nombre de grilles derrière le cylindre. Une fréquence propre de développement des tourbillons est expérimentalement déterminée et elle est expliquée par l'instabilité de la couche séparée sur le flanc du cylindre.

## GRUNDLEGENDE UNTERSUCHUNG DER SYMMETRISCHEN WIRBELERZEUGUNG HINTER EINEM ZYLINDER

**Zusammenfassung**—Der Mechanismus der symmetrischen Wirbelausbildung hinter einem Zylinder in einer gleichförmigen Aufwärtsströmung durch Beheizung des Nachlaufes mit feinen Drähten oder durch Anbringen einer geschlitzten Platte oder eines Gitters wird experimentell untersucht. Im Falle der Beheizung des Nachlaufes geht die Wirbelform bei ansteigender Wärmezufuhr von Karman-Wirbelstraßen allmählich in symmetrische Wirbel über. Ähnliche symmetrische Wirbelausbildung wird außerdem durch Anwachsen der Plattenlänge oder der Maschenzahl hinter dem Zylinder beobachtet. Eine Eigenfrequenz der symmetrischen Wirbelausbildung wird experimentell bestimmt und sie wird durch eine Instabilität der Scherungsschicht, losgelöst auf der Seite des Zylinders, erklärt.



**ФУНДАМЕНТАЛЬНОЕ ИССЛЕДОВАНИЕ ГЕНЕРИРОВАНИЯ СИММЕТРИЧНЫХ  
ВИХРЕЙ ЗА ЦИЛИНДРОМ ЗА СЧЕТ НАГРЕВА СЛЕДА ИЛИ  
РАСЩЕПЛЯЮЩЕЙ ПОТОК ПЛАСТИНЫ ИЛИ СЕТКИ**

**Аннотация**—Экспериментально изучается механизм срыва симметричного вихря за цилиндром в однородном потоке за счет нагрева следа тонкими проволочками или расщепляющей поток пластины или сетки. В случае нагрева следа при увеличении подвода тепла вихревая структура постепенно изменяется от вихревых дорожек Кармана до симметричных вихрей. Подобный отрыв симметричных вихрей наблюдался также при увеличении длины расщепляющей пластины или числа ячеек сетки за цилиндром. Собственная частота срыва симметричного вихря определена экспериментально и объяснена существованием неустойчивости сдвигового слоя, отделяющегося со стороны цилиндра.